Methodology for Calculation of Scattering Parameters in a Transmission-Line Transducer

Edval J. P. Santos and Leonardo B. M. Silva
Laboratory for Devices and Nanostructures, Departamento de Eletrônica e Sistemas,
Universidade Federal de Pernambuco. Rua Acadêmico Hélio Ramos, s/n, Várzea, 50740-530, Recife, PE, Brasil.
Email: edval@ee.ufpe.br, Ph./Fax: +55(81)2126-8214

Abstract: Transmission-line transducers are used for the measurement of absorption and reflection of different materials, such as: liquids, granular medium, and ground. A simplified methodology for calculation of scattering parameters of such transducers is presented. The transducer cell is partitioned at each interface and the partial scattering equations are calculated, considering two interfaces at a time. Next, standard techniques are applied to solve the signal-flow diagrams to obtain the full scattering equations. The proposed methodology has been applied to a coaxial transducer cell filled with different low-loss liquids. The results have been confirmed with computer simulations and experimental measurements. Measurements and simulations were carried out in the 300 kHz to 3 GHz frequency range.

Keywords: S-parameter, transmission-line transducer, multiple interface, passive device.

1. Introduction

Transmission-line transducer cells are very much used in the characterization of different materials, both liquids and solids. By measuring the S-parameters, one can extract the complex permeability and permittivity using the NRW algorithm [1,2,3,4,5,6,7,8]. However, the calculation of scattering parameters in a multiple interface coaxial cell is a daunting task. Impedance mismatch at the interfaces results in partial reflections of the incoming signal. Multiple reflections and transmissions occurs at each interface. Besides, wall surface absorption, possible non-linearity with increased power, and evanescent modes adds to the difficulty. Thus, the goal of obtaining theoretical expressions for the complete device is not practical, as the signal-flow diagram becomes quite complex. The resulting expressions are hard to analyze and the contributions of a particular interface is difficult to isolate. Computer programs can be used to simulate transmission and reflection for the complete device. But analytical expressions

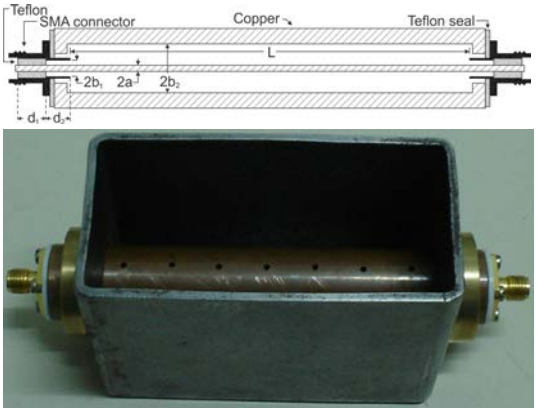

Figure 1. Transducer cell to demonstrate the proposed methodology.

are useful to give further insight into the transducer design.

In this paper, a simplified approach is presented to make this calculation feasible, and a detailed calculation is performed for a coaxial transducer cell with four interfaces. The resulting expressions are compared to measurement data and simulation. The measurement is carried out with a vector network analyzer. The simulation was performed with COMSOL Multiphysics® 4.1a, a finite element package [9]. The S-parameters are obtained in the 300 kHz to 3 GHz frequency range.

This paper is divided into four sections. This introduction is the first. Next, the coaxial transducer cell design is presented, the solution of the proposed signal flow diagram, the computation model, and low- and high-frequency measurements are described. In section 3, the results and analysis are presented. Finally, the conclusions.

2. Methodology

2.1 Coaxial transducer cell design

A two-port coaxial transducer cell with four interfaces is used to demonstrate the proposed methodology. The designed and machined coaxial line is presented in Figure 1 [5]. Five sections and four interfaces are identified, as

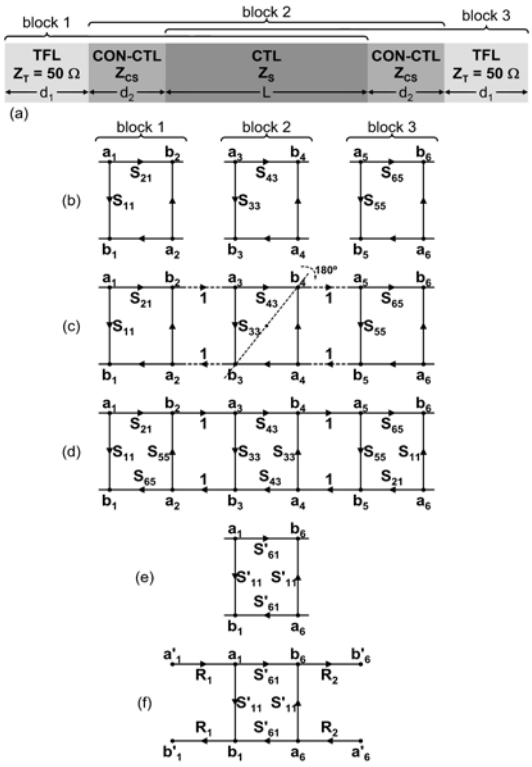

Figure 2. Coaxial cell section modelling to build the signal flow diagram. (a) The transmission line is divided into five sections. (b) S-parameters for blocks 1, 2 and 3. (c) At the block interfaces, it is assumed perfect transmission. (d) Proposed signal flow diagram. (e) Resulting two-port network. (f) The reference plane transformation factors, R_1 and R_2, are introduced.

shown in Figure 2. The center section can be filled with a liquid to modifiy the permittivitty. The connectors at both ends are 703-model SMA-connector [10], and can modelled as two-section elements, of lengths: d_1 and d_2. The first section with length d_1 = 6.6 mm is a coaxial element filled with teflon. It is a transition region connected to the cable from the network analyzer. The second section has the same dielectric as the transmission line itself. This region has a length d_2 = 5.6 mm, and a diameter $2b_1$ = 3.7 mm. The center section of the coaxial cell has a length L = 92.6 mm, and the central wire has a diameter, $2a$ = 1.35 mm, which is the same in the connectors and in the cell. The coaxial cell has an internal diameter $2b_2$ = 11.2 mm.

The first section of the connector, filled with teflon, is assumed to have an impedance Z_T = 50 Ω. The impedance of the second section is given by Equation 1.

$$Z_{CS} = 60\sqrt{\frac{\mu_r}{\varepsilon_r}}\ln\left(\frac{b_1}{a}\right) \qquad (1)$$

where $\varepsilon_r = \varepsilon_r' - j\varepsilon_r''$ and $\mu_r = \mu_r' - j\mu_r''$ are respectively the relative complex permittivity and complex permeability of the sample.

The third section corresponds to the transducer cell. It is a transmission line with impedance given by Equation 2.

$$Z_S = 60\sqrt{\frac{\mu_r}{\varepsilon_r}}\ln\left(\frac{b_2}{a}\right) \qquad (2)$$

For the designed passive device, when the coaxial line is filled with air the characteristic impedance is Z_S = 127 Ω. The fourth and fifth sections are equal to the first two in reverse order.

The first half of the connector is the region named TFL; the second half is the region named CON-CTL. The transducer cell section is named CTL. The first and last regions are assumed to be matched to the cables, and are modelled as a phase displacement. The other three sections are modelled with a signal flow diagram, as presented in Figure 2(a).

2.2 Solving the signal-flow diagram

To solve the signal-flow diagram for the complete cell is a dauting task. Depending on the level of mismatch, there will be infinite reflections in all interfaces. The simplification proposed in this paper is to consider two interfaces at a time. As the test transducer cell can be divided into five regions, there will be three two-interface blocks.

- Block 1: TFL/CON-CTL/CTL.
- Block 2: CON-CTL/CTL/CON-CTL.
- Block 3: CTL/CON-CTL/TFL.

The coaxial structure supports the *TEM* mode. Neglecting evanescent waves at the region boundaries and assuming perfect conductivity at the metal surfaces, the *TEM* mode propagation can be calculated with conventional circuit analysis [11]. The transmission/reflection analysis is carried out for each block.

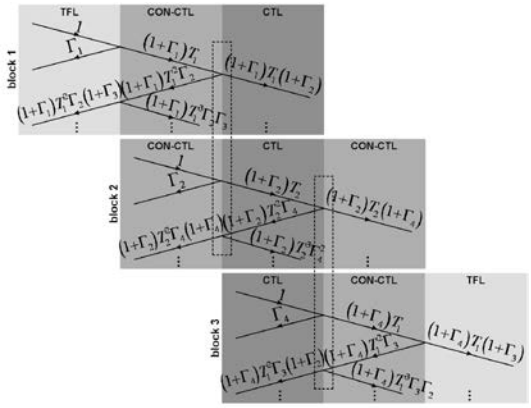

Figure 3. Diagram illustrating the approach used to calculate the partial S-parameters of the coaxial cell. The cell is divided into three blocks for the calculation. The dashed line indicates the interfaces which are accounted twice.

Considering the first block, Γ_1 is the reflection coefficient at the interface TFL/CON-CTL. The transmission coefficient at this interface is given by $1 + \Gamma_1$. As the wave travels in the dielectric inside the region CON-CTL, some energy is absorbed. To account for such absorption, a transmission coefficient T_1 is introduced [12,13]. As the transmitted signal reaches the interface CON-CTL/CTL a new reflection, with coefficient Γ_2, and a new transmission, with coefficient $1 + \Gamma_2$, occurs. The reflected signal in the region CON-CTL reaches the interface TFL/CON-CTL and the same behavior is observed, but now the reflection coefficient is given by Γ_3. This process continues indefinitely, as illustrated in Figure 3. Similarly, T_2 is defined to account for energy absorption in the CTL region.

The reflection coefficients are given by

$$\Gamma_1 = \frac{Z_{CS} - Z_T}{Z_{CS} + Z_T} = -\Gamma_3 \tag{3}$$

$$\Gamma_2 = \frac{Z_S - Z_{CS}}{Z_S + Z_{CS}} = -\Gamma_4 \tag{4}$$

$$\Gamma_3 = \frac{Z_T - Z_{CS}}{Z_T + Z_{CS}} = -\Gamma_1 \tag{5}$$

For a low-loss dielectric sample, and neglecting conductor losses, the transmission coefficients can be written as

$$T_1 = e^{-\gamma d_2} \tag{6}$$

$$T_2 = e^{-\gamma L} \tag{7}$$

where d_2 is the CON-SAM region length, L is the SAMPLE region length.

$$\gamma = j\frac{2\pi}{c}\sqrt{\varepsilon_r \mu_r}\, f \tag{8}$$

where γ is the propagation constant in the device, c is the speed of light in vacuum and f is the frequency.

As can be observed in Figure 3, the division into blocks introduces an error, as two interfaces are accounted twice in the calculation of the reflection coefficient of the complete device. Hence, the resulting reflection coefficient is twice the correct value. To compensate for this, a correcting factor of 2 is introduced in the reflection coefficient, $\Gamma_2' = \Gamma_2/2$. Thus removing the double count at the CON-CTL/CTL and CTL/CON-CTL interfaces. Adding up all reflections, Equation 9 is obtained. Similarly, all transmitted wave components at the second interface in Block 1 are summed up. The procedure is repeated for Blocks 2 and 3, to obtain all the required S-parameters.

$$S_{11} = \frac{\Gamma_1 + \Gamma_2' T_1^2}{1 + \Gamma_1 \Gamma_2' T_1^2} \tag{9}$$

$$S_{21} = \frac{(1+\Gamma_1)(1+\Gamma_2')T_1}{1 + \Gamma_1 \Gamma_2' T_1^2} \tag{10}$$

$$S_{33} = \frac{\Gamma_2'\left(1 - T_2^2\right)}{1 - \Gamma_2'^2 T_2^2} \tag{11}$$

$$S_{43} = \frac{T_2\left(1 - \Gamma_2'^2\right)}{1 - \Gamma_2'^2 T_2^2} \tag{12}$$

$$S_{55} = -\frac{\Gamma_2' + \Gamma_1 T_1^2}{1 + \Gamma_1 \Gamma_2' T_1^2} \tag{13}$$

$$S_{65} = \frac{(1-\Gamma_1)(1-\Gamma_2')T_1}{1 + \Gamma_1 \Gamma_2' T_1^2} \tag{14}$$

where, $\Gamma_2' = \Gamma_2/2$.

Using the fact that the device is symmetric, the signal-flow is the same if a 180° rotation is performed, as indicated in Figure 2(c). The complete signal-flow diagram is presented in Figure 2(d). The resulting diagram can be solved with the non-touching loop rule [14] or Mason's decomposition rules. The results are presented in Equations 15 and 16, see Figure 2(e).

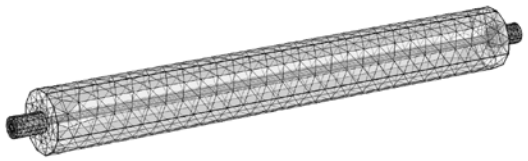

Figure 4. Geometry for the coaxial transmission line with the same dimensions as the real device as designed in COMSOL Multiphysics.

$$S'_{11} = S_{11} + \frac{S_{21}S_{33}S_{65}\left(1-S_{33}S_{55}\right)+S_{21}S_{43}^2S_{55}S_{65}}{\left(1-S_{33}S_{55}\right)^2+S_{55}^2S_{43}^2} \quad (15)$$

$$S'_{61} = \frac{S_{21}S_{43}S_{65}}{\left(1-S_{33}S_{55}\right)^2-S_{55}^2S_{43}^2} \quad (16)$$

It can be verified that the network is reciprocal, i.e.,

$$S'_{1i}S'^{\,*}_{1j} + S'_{6i}S'^{\,*}_{6j} = \delta_{ij} \quad (17)$$

where δ_{ij} is the Kronecker delta symbol.

Finally, the reference plane transformation factors, R_1 and R_2, are introduced, see Figure 2(f). These factors account for any eventual error in the scattering parameter phase due to the use of connectors/adapters or calibration errors that occurs in practice.

$$S^{\dagger}_{11} = R_1^2 S'_{11} \quad (18)$$

$$S^{\dagger}_{61} = R_1 R_2 S'_{61} \quad (19)$$

where

$$R_1 = e^{-\gamma_0 L_1} \quad (20)$$

$$R_2 = e^{-\gamma_0 L_2} \quad (21)$$

where γ_0 is the propagation constant in the region between the calibration plane and the sample. L_1 is the distance between the first calibration reference plane and the sample and L_2 is the distance between the second calibration reference plane and the sample.

2.3 Computational model

The transducer cell was modelled and simulated in COMSOL Multiphysics® 4.1a simulation software [9]. The model is a combination of three cylindrical bodies, representing the external conductor, and one cylindrical body, representing the internal conductor. A dielectric material is defined in the region between the outside and the inside cylinders, as shown in Figure 4. This model is equivalent to Block 2, CON-CTL/CTL/CON-CTL. At both ends, lumped ports are defined as coaxial elements with a 50 Ω characteristic impedance.

Table 1: Capacitance and relative permittivity measurements.

Sample	C (pF)	C_{meas} (PF)	ε_r' (literature)	ε_r' (by capacitance)
Air	4.689	4.64	1.000 [17]	0.984
N-pentane	7.161	7.35	1.837 [17]	1.872
N-hexane	7.405	7.76	1.892 [17]	2.006
Turpentine	8.351	8.36	2.3 [18]	2.203

The lumped ports act as semi-infinite cables, thus the calibration planes are set at these interfaces. The material surfaces are defined to be copper with zero tangential electric field component, $\vec{n}\times\vec{E}=0$. Different dielectric are simulated by modifying the relative permittivity between the conductors. After geometry and materials definition, the finite element mesh is generated, as shown in Figure 4. Mesh size is chosen to be at least five times smaller than the smallest wavelength of the propagating electromagnetic wave. Next to the ports, finer mesh is generated. Simulation in COMSOL is carried out at 51 frequency values, in the 10 MHz to 3 GHz frequency range. The simulation is performed using the Time-Harmonic Electromagnetic-wave Physics interface to obtain the S-parameters. Examples of simulations related to this work can be found in references [15,16].

2.4 Low-frequency measurements

Using non-polar liquids, low frequency measurements were performed to get the permittivity. For such liquids, the permittivity does not change much with frequency. Capacitance measurements were perfomed at 10 kHz with a Stanford Research 720 impedance meter. The results are presented in Table 1.

This causes an error in the high-frequency range fitting of the transmission data. To improve the match an extraction of the permittivity in the full frequency range is required. Also, one has to take into account to the cable mismatch, and the finite conductance of the metal used in the cell fabrication.

2.5 High-frequency measurements

The S-parameter measurement is performed with the Agilent 8714T vector network analyzer, in

Table 2: Key electrical data for different sample materials.

Sample	Z_{CS} (Ω)	Z_S (Ω)	Γ_1	Γ_2	λ_{min} (cm)
Air	60.98	127.97	0.099	0.355	10.1
N-pentane	44.21	92.78	-0.061	0.355	7.3
N-hexane	42.71	89.63	-0.079	0.355	7.1
Turpentine	40.75	85.53	-0.102	0.355	6.7

the 300 kHz to 3 GHz frequency range. The connection between the network analyzer ports and the coaxial cell is made with a type-N(m)/SMA(f) adapter followed by a 25 cm SMA-cable with male connectors.

In Table 2, key data used in the calculations are presented. From this table, one can see that Γ_2 does not depend on the sample analyzed, it is a function of the geometry of the coaxial transmission line.

The full two-port calibration is performed using an appropriate SMA-kit. The calibration reference plane for S_{11}' is at the end of the reflection SMA-cable. For the S_{61}' calibration, the cables are connected together, making a short-circuit between the network analyzer ports, one additional adapter is required to complete this connection. After calibration, the adapters are removed from the cables, and the system is ready.

3. Results and analysis

The cell is mounted in a box made of brass, the liquid to be analyzed is poured into this box and penetrates the cell through holes made along the external cylinder. The hole diameter is much smaller than the wavelength, so that they do not affect the cell impedance characteristics. This has been confirmed by measurement, as the S-parameters measurements before and after hole perforation display no noticeable difference. The transducer cell is inserted into the brass box through lateral holes made specifically for this purpose. In these holes rubber o-rings are used to avoid leakage.

For the S_{11}' measurements, one end of the transducer cell is connected to the reflection port in the network analyzer with an SMA-cable, and the other end is connected to a 50 Ω load, so unwanted reflections are avoided. At some particular frequencies, the sample length is a multiple of half-wavelength of the input signal, see Equation 22. At such frequencies, reflection becomes very small, and transmission is maximum. With different dielectric materials in the sample region, the speed of light changes, consequently the resonance positions also changes.

$$L + 2d_{2,e} = n\frac{\lambda}{2} = \frac{c}{2f\sqrt{\varepsilon_r \mu_r}} \qquad (22)$$

where $0 < d_{2,e} < d_2$ is the effective length of the region inside the connector with the same dielectric as the transmission line.

As an indication that Equations 18 and 19 are correct, one can make a simplification by forcing $\Gamma_2' = 0$ and $T_1 = 1$. The resulting expressions as presented in Equations 23 and 24, that are well known from the literature [1,3].

$$S_{11}^{\dagger\dagger} = R_1^2\left[\frac{\Gamma\left(1-T^2\right)}{1-\Gamma^2T^2}\right] \qquad (23)$$

$$S_{61}^{\dagger\dagger} = R_1R_2\left[\frac{T\left(1-\Gamma^2\right)}{1-\Gamma^2T^2}\right] \qquad (24)$$

where $\Gamma = \Gamma_1$ and $T = T_2$.

The combined plot of the experimental data, simulation results, and theoretical expression for S_{11}' and S_{61}' for different dielectric materials are presented in Figure 5. As can be seen, the methodology proposed yields expressions which fits quite well the experimental and simulated data.

Transmission measurements of $|S_{61}'|_{dB}$, shown in Figure 5 top-right, display some oscillations, this is due to the mismatch in the region of the cable connecting the cell to the transmission port of the network analyzer. The agreement may be improved by adjusting γ in Equation 8 to account for the medium absorption (α_d) and the finite conductance at the cell surface (α_c), as shown in Equation 25 [19]. Neglecting losses due to radiation, and losses due to medium conductivity.

$$\gamma(f) = \left[\alpha_d(f) + \alpha_c(f)\right] + j\beta \qquad (25)$$

where,

$$\alpha_d(f) = \frac{\sqrt{\varepsilon_r'\mu_r'}}{c}\left[\frac{1}{2}\sqrt{1+\tan^2\delta} - \frac{1}{2}\right]^{1/2} 2\pi f$$

$$\alpha_c(f) = \sqrt{\varepsilon_r'}\left[\sqrt{\frac{\varepsilon_0}{8\sigma}}\frac{a+b}{ab}\frac{1}{\ln(b/a)}\right]\sqrt{2\pi f}$$

where, $tan\,\delta$ is the loss tangent, and σ is the conductivity of copper, which is $5.9773 \times 10^7\ \Omega^{-1}m^{-1}$ at 293 K [20].

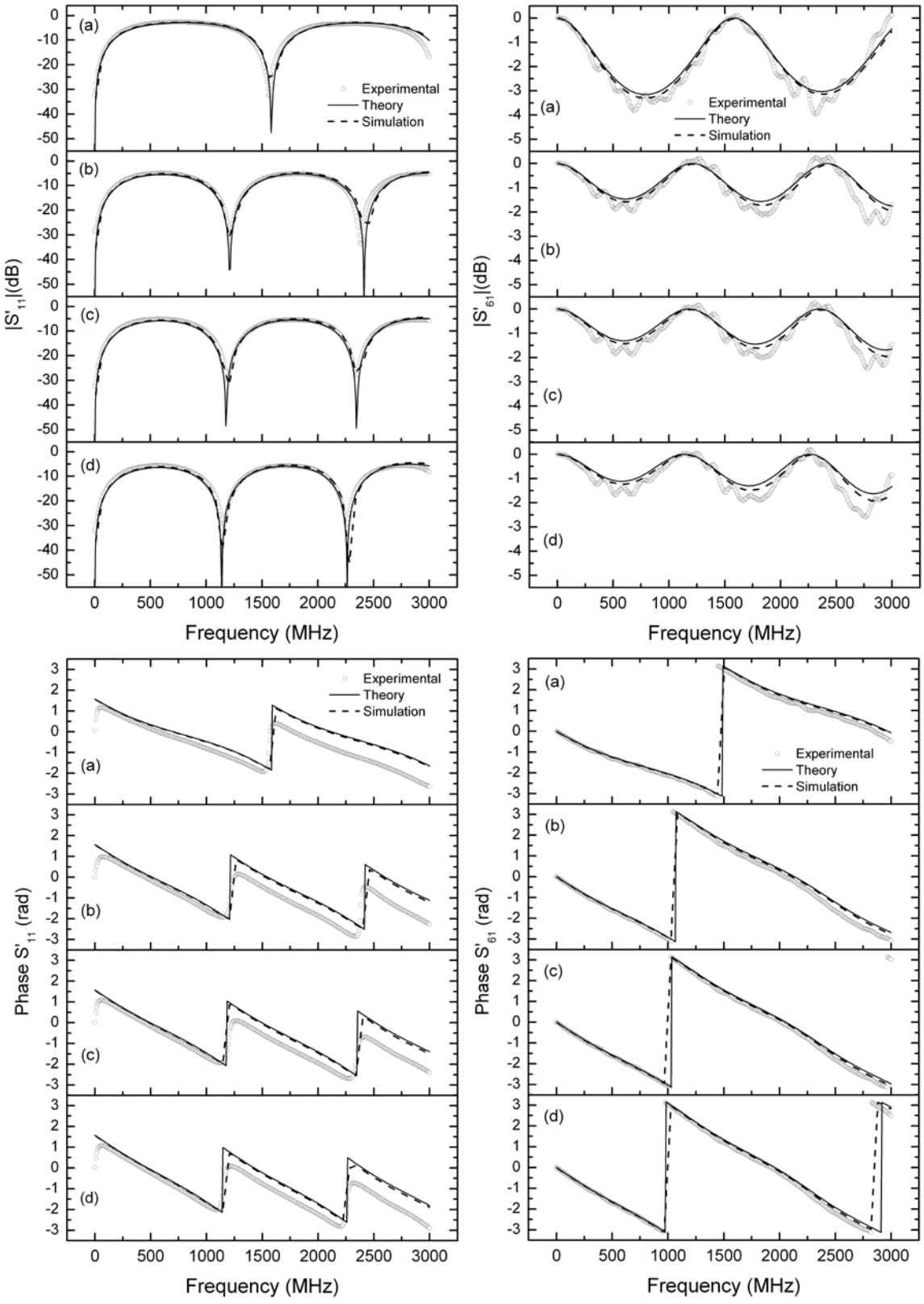

Figure 5. S-parameters for the cell filled with (a) air, (b) n-pentane, (c) n-hexane and (d) turpentine.

4. Conclusions

The proposed methodology to obtain theoretical expressions of the scattering parameters for a multiple interface transducer cell has been validated for a coaxial transmission line with five regions. The obtained expressions fits well the experimental and simulated data.

To demonstrate the methodology, a low frequency dielectric constant of non-polar fluids is used. This causes an error in the high-frequency range fitting of the transmission data. To improve the match an extraction of the permittivity in the full frequency range is required. Also, one has to take into account to the cable mismatch, and the finite conductance of the metal used in the cell fabrication.

The resulting expressions also reduces to the well known expressions found in the literature for simpler devices. Next step is to validate the methodology to more complex geometries, such as a seven region coaxial line.

5. References

1. J. Baker-Jarvis, E. Vanzura, and W. Kissick, Improved technique for determining complex permittivity with the transmission/reflection method, *IEEE Transactions on Microwave Theory and Techniques*, **38**, 1096-1103 (1990).
2. J. Baker-Jarvis, M. D. Janezic, and C. A. Jones, Shielded open-circuited sample holder for dielectric measurements of solids and liquids, *IEEE Transactions on Instrumentation and Measurement*, **47**, 338-342 (1998).
3. K. C. Lawrence, S. O. Nelson, and P. G. Bartley, Flow-through coaxial sample holder design for dielectric properties measurements from 1 to 350 MHz, *IEEE Transactions on Instrumentation and Measurement*, **47**, 354-361 (1998).
4. K. J. Bois, L. F. Handjojo, A. D. Benally, K. Mubarak, and R. Zoughi, Dielectric plug-loaded two-port transmission line measurement technique for dielectric property characterization of granular and liquid materials, *IEEE Transactions on Instrumentation and Measurement*, **48**, 1141-1148 (1999).
5. L. B. M. Silva and E. J. P. Santos, Modified NRW Algorithm for Unmatched Cell, in *Proceedings of the International Microwave and Optoeletronics Conference - IMOC 2009*, Belém, Brasil, 2009.
6. R. Bhunjun and Rolf W. Vogt, Sensor system for contactless and online moisture measurements, I*EEE Transactions on Instrumentation and Measurement*, **59**, 3034-3040 (2010).
7. C. Larsson, D. Sjöberg, and L. Elmkvist, Waveguide measurements of the permittivity and permeability at temperatures of up to 1000°C, *IEEE Transactions on Instrumentation and Measurement*, **60**, 2872-2880 (2011).
8. D. Zhao, G. Rietveld, G. M. Teunisse, A multistep approach for accurate permittivity measurements of liquids using a transmission line method, *IEEE Transactions on Instrumentation and Measurement*, **60**, 2267-2274 (2011).
9. COMSOL (http://www.comsol.com).
10. http://www.temple-star.com/sma_kabel_connector_mil_c_39012.htm.
11. L. F. Chen, C. K. Ong, C. P. Neo, V. V. Varadan, and V. K. Varadan. *Microwave Electronics: Measurement and Materials Characterization.* John Wiley & Sons (2004).
12. C. Courtney, W. Motil, T. Bowen, and S. Blocher, Measurement Methods and the Characterization of the Electromagnetic Properties of Materials, *U.S. Air Force Research Laboratory Directed Energy Directorate, Kirtland AFB, NM, Measurement Notes 48* (1996).
13. N. Patel, Theory, simulation, fabrication and testing of double negative and epsilon near zero metamaterials for microwave applications, *Faculty of California Polytechnic State University, San Luis Obispo, Master thesis* (2008).
14. Agilent AN 154, S-Parameter Design, Application Note.
15. S. M. Musa and M. N. O. Sadiku, Analysis of Rectangular Coaxial Lines, *Region 5 Technical Conference IEEE* (2005).
16. J. P. kaerst, Resonances in tapered double-port TEM waveguides, *Excerpt from the Proceedings of the COMSOL Conference 2008 Hannover*.
17. D. R. Lide, *CRC Handbook of Chemistry and Physics*. 87th ed. Editor-in-Chief (2006).
18. M. A. Laughton and D. J. Warne, *Electrical Engineer's Reference Book*. Elsevier Science (2003).
19. E. J. P. Santos, Determination of Ethanol Content in Gasoline: Theory and Experiment, in *Proceedings of the International Microwave and Optoeletronics Conference - IMOC 2003*, 349-353, Foz do Iguaçu, Brasil (2003).
20. J. Emsley, *The Elements*, Oxford, Clarendon Press (1989).

6. Acknowledgements

The authors thank Mr. Antonio J. P. Menezes for his help with the transducer fabrication. Thanks to CNPq, and FINEP, brazilian agencies, for their continued support.